J. Astrophys. Astr. (1987) **8**, 195–209

Evolution of the Optical Spectrum of SN 1987a in the Large Magellanic Cloud

B. N. Ashoka, G. C. Anupama, T. P. Prabhu, S. Giridhar,
K. K. Ghosh, S. K. Jain, A. K. Pati & N. Kameswara Rao
Indian Institute of Astrophysics, Bangalore 560034

Received 1987 April 13; accepted 1987 April 29

Abstract. The evolution of the spectrum of SN1987a is traced from 1987 February 26 to March 31. Based on the low-resolution spectroscopic data we identify the lines of H, He I, Na I, Fe II, Sc II, Ca II which are known to be present in Type II Supernovae, and also present evidence for the existence of lines of Mg I, Ca I, O I, and N I. We discuss the evolution of the Hα profile, and draw attention to its complex structure around March 30. Close to the rest wavelength of Hα a double-peaked structure appeared in the profile with a peak-to-peak separation of ~ 1400 km s^{-1}, suggestive of an expanding shell or disc of gas.

Using the available broadband photometric information, we also trace the evolution of the photosphere of SN1987a assuming that it radiates like a supergiant.

Key words: Supernovae, spectra—Supernovae, SN1987a

1. Introduction

Supernova (SN) 1987a in the Large Magellanic Cloud (LMC) was discovered on 1987 February 24 at a brightness of m_v = 4.5 (*IAU Circular No.* 4316). Its dramatic rise did not continue for long, and the light curve levelled off initially at about m_v = 4.3, and then began a slow rise by ~ 0.017 mag day^{-1}.

Though the optical spectrum of SN 1987a showed characteristics similar to a typical Type II, the supernova was peculiar in many respects. In the optical region, the striking deviations from a typical supernova are in terms of very high absorption velocities of Balmer lines during the early phases, and a peculiar light curve.

The observations of SN 1987a commenced at the Vainu Bappu Observatory (VBO) Kavalur (latitude = 12°34′), on 1987 February 26. Some spectroscopic measurements have been communicated through (*IAU Circular Nos* 4339, 4340, 4359). We present here a brief description of the nature and evolution of the spectrum between 1987 February 26 and March 31. We also discuss the photometric behaviour based on data gathered mostly from *IAU Circulars.*

2. Observations and reductions

We monitored the spectrum of SN 1987a at reciprocal dispersions ranging from 100 to 250 Å mm^{-1} over a wavelength range of $\lambda\lambda$4000–9000 (wavelengths are expressed in Å units all through). Spectrograms were obtained regularly with the Bhavanagar spectrograph using gratings of 300 and 400 grooves mm^{-1} and a 75-mm camera, at the Cassegrain focus of the 0.75-m reflector. In addition, some spectrograms were obtained also at the Cassegrain focus of the 1-m reflector with the help of Carl-Zeiss UAG spectrograph, using a grating of 651 grooves mm^{-1} and a 110-mm camera. Kodak 098-02 and I-N (hypersensitized) emulsions were employed. Occasionally, a 150-mm camera was used in conjunction with a Varo 8605, single-stage, electrostatistically-focussed image tube and spectra were recorded on Kodak IIa-D plates. All plates were calibrated for relative intensity using an auxilliary calibration spectrograph. A few photoelectric spectrum scans were also obtained with a bandpass of 50 Å at the Cassegrain focus of the 1-m reflector.

The spectrograms were digitized using PDS-1010M microdensitometer, generally at a speed of 2 mm s^{-1}, using a sampling interval of 5 μm. RESPECT software (Prabhu, Anupama & Giridhar 1987) was used for final reductions, though some of the preliminary measurements reported here have been made directly on an auxiliary analogue chart output of the microdensitometer. The interactive reductions using RESPECT software include smoothing by a low-pass filter (cut-off frequency ~15 cycles mm^{-1}), and conversion to intensity scale achieved through the characteristic curve determined as a polynomial of third degree in Baker-transformed densities. The wavelength scale was established as a polynomial using the laboratory comparison spectrum (Fe + Ar or Fe + Ne hollow cathode source) exposed on both sides of the spectrum. The spectra were linearized in wavelength through natural cubic-spline interpolation at regular intervals in wavelength.

3. Optical spectrum and its evolution

The spectrum of SN 1987a conforms to the general characteristics of SN II with hydrogen lines in emission although it is not a typical Type II. Since the time of rapid rise to 4.5 mag on February 24–25, the spectrum evolved from a Balmer-line-dominated one with broad P-Cygni type emission to one with strong blue-shifted absorption features due mostly to Fe II and Na I.

Following Patchett & Branch (1972) we use the absorption features as more reliable means of identification. As pointed out by Kirshner *et al.* (1973), the features in both Type I and Type II Supernovae are essentially the same; hence, the identifications of features in Type I SN 1981b in NGC 4536 (Branch *et al.* 1983), and in Type II SN 1979c in M 100 (Branch *et al.* 1981) were used as a guide. The dominant species identified are due to H, He I, Na I, Fe II, Mg I and perhaps Sc II.

3.1 *The Early Spectrum*

Our first spectrum recorded on February 26.63 (Fig. 1) shows broad Hα emission with strong P-Cygni absorption at a velocity of – 16400 km s^{-1}. The absorption compo-

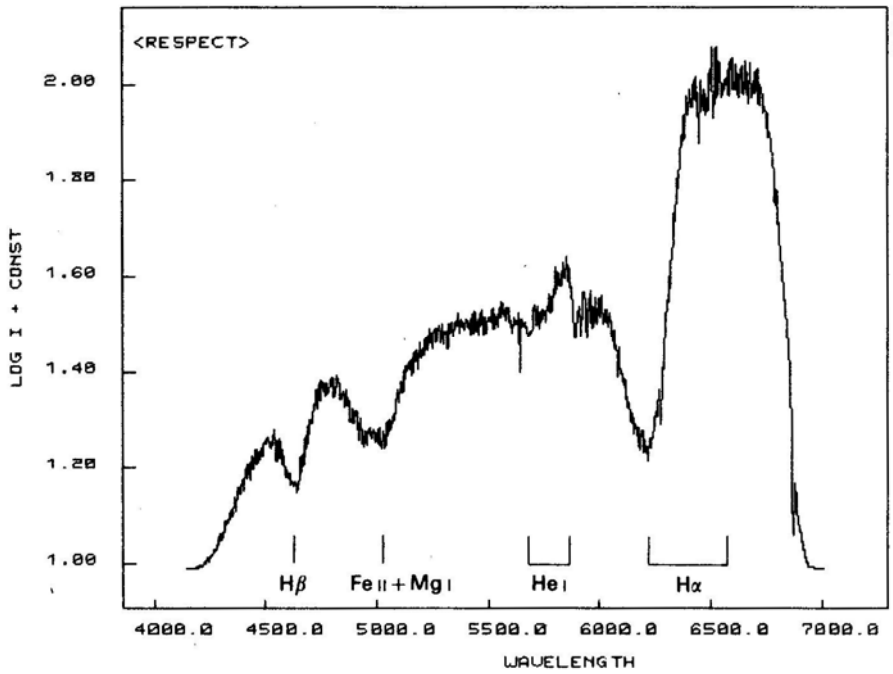

Figure 1. The spectrum of SN 1987a recorded on 1987 February 26.63 at 110 Å mm^{-1} The sharp feature at λ5650 is a plate flaw. The correction for instrumental response has not been applied.

nent reaches the continuum only at – 25500 km s^{-1}. The continuum is fairly strong. We attribute the P-Cygni feature at λ5900 to He I λ5876 instead of Na I D since the latter is not expected to be seen so early in the evolution of the supernova. The absorption velocity of this line is at – 9400 km s^{-1}, considerably smaller in magnitude than the value for Hα. The emission component is severely distorted by interstellar Na I D, and atmospheric absorption lines. He I λ6678 is possibly blended with Hα. Other strong lines in the spectrum are Fe II + Mg I blend at λ5176, and Hβ. The blend at λ5176 has an absorption velocity similar to that of He I whereas the corresponding value of Hβ (– 13000 km s^{-1}) lies in between these and Hα.

The first near-infrared spectrum recorded on February 27.62 shows the Ca II triplet at λ8600 prominently. The P-Cygni absorption is, however, blended with atmospheric absorption due to H_2O. The estimated absorption core velocity was –7900 km s^{-1}, similar to He I and λ5176 features. Some of our early spectra are shown in Fig. 2.

3.2 *Evolution of the Spectrum*

The most striking change in the spectrum of SN 1987a during the period of observation is the continuous decrease of the magnitude of absorption velocity. The measured velocities of different lines and blends are listed in Table 1, and are plotted in Fig. 3. The spectrum also moves continuously to lower excitation and lines of Na I and Fe II begin

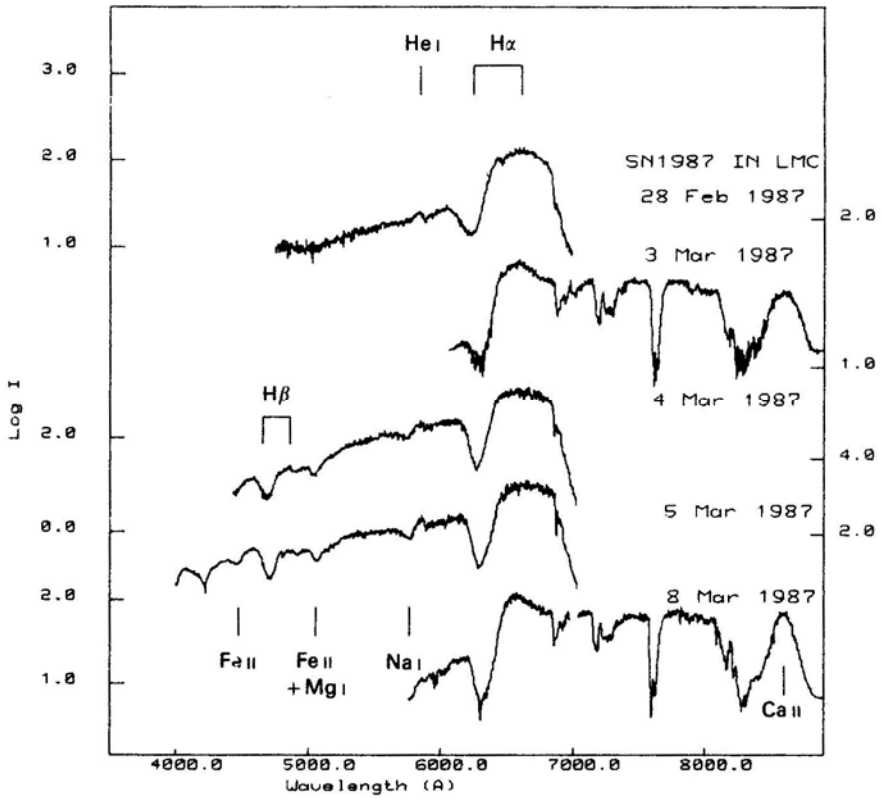

Figure 2. Early spectra of SN 1987a, not corrected for instrumental response. The scale marks alternate between left and right.

to appear and strengthen. We discuss in the following these changes in lines of individual species.

3.2.1 *The Balmer Lines*

The profiles of Balmer lines show flat-bottomed P-Cygni absorption until about March 8 indicating high optical depths. Initially the amount of absorption was roughly equal to emission. With time the absorption component narrowed down and the emission increased relative to absorption. The profile of March 3 compared to that of March 8 in Fig. 4 exemplifies these changes. The peak of the emission component was initially shifted to shorter wavelengths compared to the rest wavelength. With time the emission peak moved toward the rest wavelength.

One can make crude estimates of the radius of the Hα-scattering envelope from the ratios of radial velocities of blue and red extremities of the profile (Kuan & Kuhi 1975). The derived extent is about 1.2 photospheric radii on March 3 and 1.3 on March 8.

The evolution of Hα absorption cannot be traced beyond March 22 due to the increasing strength of P-Cygni profile of Fe II λ6456. A dramatic change in the emission

Table 1. Radical velocities (km s^{-1}) of blueshifted absroption features.

Date 1987	4100 Hδ	4340 Hγ	"4568" Fe II	4861 Hβ	4924 Fe II	5018 Fe II	"5176"	5325.56 Fe II	5535 Fe II	"5675"	5876 He I	5892 Na I	"6135" Fe II	"6263" Fe II	6456 Fe II	6563 Hα
February 26				13000			8600				9400					16400
February 28											7400					14800
March 2			7700	11000		8100	8200					7300				13800
March 3																
March 4			8400	11000		6900	8100		8300			7800				13400
March 5	7800	9000	7400	9800	7400	6500	6600	6200		7500		6600				12300
March 6			7700	9700	6500	6600	6700		6900			6500	5900			12200
March 8		7100	6800	8000	5300	5400	5400	5600	5300	5300		5500	5300	5200		10400
March 9					5400			4300	4800	5400		5500	5100			10300
March 13					4900	4400	4700	4300	4400	4500		4500	4400	4400		9300
March 14									4200	4200		4700	3800			8800
March 15									3700	4100		4700	3700	3900		8300
March 16					3300	3800	3300	3900	3900	4000		4400	3700	3400		8300
March 19					4300	3400	3300	3500	3600	3700		4100	3400	3400		8000
March 22									2700	2800		4200	3200	3100	2800	7700
March 23						3400	4000		3600	3600		4000	3500	3500	3000	
March 25					3200	3000	2900	2200	3200	3300		3700	3600	3200	2800	
March 26						3000	3200	2700	3000	3200		3600		3300	2700	
March 27							3000	2600	3100	3100		4100	3200	2800	2600	
March 29									3200	3100		4200	3400	2400	2500	
March 30										3100		3900	3400	2900	2400	

Velocities are corrected for the radial velocity of LMC. Typical errors are 200 km s^{-1}.

The quotation marks denote the wavelengths of blends: Fe II "4568": 4584, 4549, 4556, 4629; "5176": 5169 of Fe II + 5183 of Mg I, "5675": Sc II (29); "6135": 6149, 6147 of Fe II, 6122 of Ca I (3) blending with Ca I seems to occur from 15 March onwards; "6263": 6248, of Fe II (74), 6280 of Sc II (28).

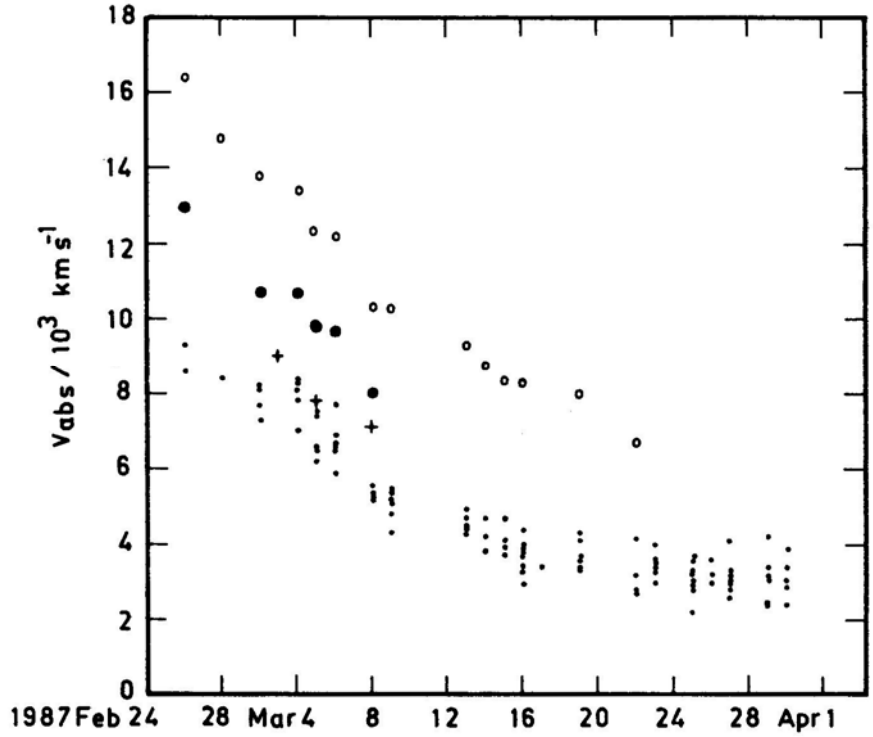

Figure 3. Absorption core velocities as a function of time. Hα: open circles; H*β*: filled circles; H*γ* and H*δ*: crosses: all other lines: dots.

profile, however, was evident on March 30. The profile had changed into a double-peaked one with the central absorption at *λ*6563 (Fig. 5): The two emission-peaks had a separation of 1400 km s^{-1} whereas the width at the base of the emission was 3150 km s^{-1}. The shape of the profile was similar to that in Be stars and novae. Particularly it is reminiscent of nova DQ Her during 1935 January-March (*of.* Fig. 9 of Beer 1973), though the peak-to-peak separation is much larger. The double-peaked Hα emission in DQ Her has been interpreted to be arising in the expanding, recombining shell between the star and the outer scattering shell (Rottenberg 1952).

There was another emission peak present at *λ*6690 since about March 22. This emission was varying in relative intensity with respect to the emission at *λλ*6538–6539. For example, on the photoelectric spectrum scan obtained on March 31 (Fig. 6) *λ*6690 appears brighter than Hα. It is tempting to ascribe this peak to He I *λ*6678. We will return to this feature again while discussing lines due to He I.

The emission due to H*β* was generally weak, though detectable on March 2.62 and 4.62. The absorption cores of Hα, H*β* and H*γ* showed velocities progressively smaller in magnitude (see Table 1).

3.2.2 *Lines due to He I*

He I *λ*5876 was conspicuous during the early evolution of the spectrum until the Na I D *λ*5892 began to dominate over it (March 2). The absorption trough of He I was

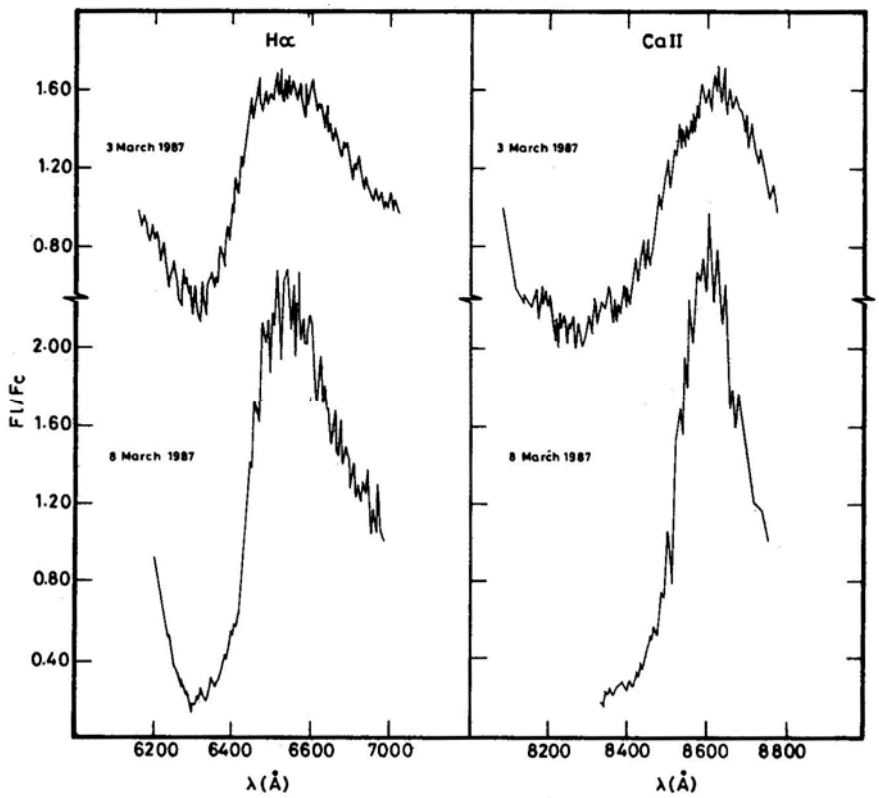

Figure 4. The change in the profiles of Hα and Ca II λ8600, reduced to an estimated continuum, on 1987 March 3 and 8.

shallower, and narrower compared to Hß. This is as expected since the optical depth of Hβ is larger than He I λ5876 at any given point in the atmosphere. The possible identification of He I λ6678 on March 30 raises the question whether the He I lines due to inner recombining shell become visible at the later phase. The other triplet transitions at λ5876 and λ7065 are, however, not very conspicuous. A sharp peak was present at λ5873 in the spectra of both March 29 and 30, superposed over the Na I D line. Some emission was evident around λ7065 on March 27 and 29. The unsmoothed data showed that the λ6678 peak was also double, but with a separation of 750–900 km s^{-1}. If the identification is right, it would imply that the velocity in the linear shell increases with radius as in the shells of novae.

3.2.3 *Lines due to Na I*

Na I D λ5893 dominated over He I λ5875 on March 2.62 and got stronger with time. Its absorption began to get flat-bottomed by March 8. An absorption feature at λ8004 possibly due to Na I $\lambda\lambda$8183, 8194 appeared on March 5 and began its redward migration. It was visible until it merged with the atmospheric absorption due to H_2O. N I (2) λ8212 may also contribute in this region.

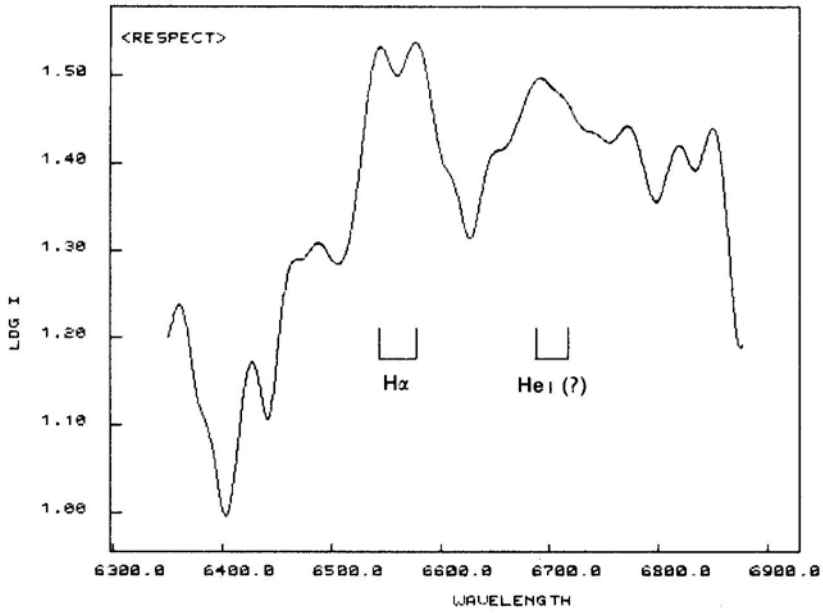

Figure 5. The region around Hα on 1987 March 30. The data has been smoothed considerably.

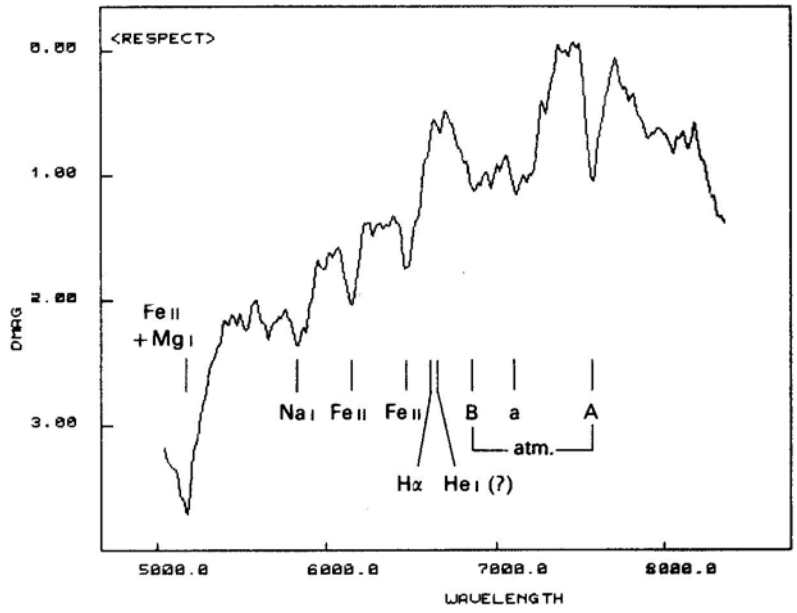

Figure 6. A photoelectric spectrum scan of SN 1987a obtained on 1987 March 31 in the range $\lambda\lambda$4800–8200 with a bandpass of 50 Å. Notice the double-peaked structure near Hα. The left peak is near λ6563, whereas the right one is near λ6678. Both the peaks are further split at higher resolutions.

When Na I D is strong we expect the lines of Mg I and K I also. Mg I λ5176 was blended with Fe II all through. The absorption due to K I $\lambda\lambda$7665, 7699 was probably blended with the blue edge of the atmospheric 'A' band. A measurable dip appeared on March 30 at λ7575 which yields absorption velocities consistent with Na I D line if ascribed to K I λ7665.

3.2.4 *Lines due to Fe II and Sc II*

The earliest Fe II lines to appear were the multiplets 38 and 42 (March 2). An absorption feature at λ5421 appeared on March 4 due to Fe II λ5535. The absorption at λ6032 seen on March 6 is due to Fe II (74) λ6148, 6149. The presence of Fe II (73) $\lambda\lambda$7449, 7462, 7515 was evident on March 8 through its absorption at λ7345 close to atmospheric 'a' band, and excess emission at 7459. There may be some contribution due to N I (3) λ7452 also here.

An absorption feature at λ7393 seen on March 22 is probably due to Fe II (73) λ7475. It implies a velocity of – 3568 km s^{-1}, consistent with other Fe II lines.

An emission feature appeared dramatically at λ6461 around March 16.62, on the red side of the P-Cygni absorption of Hα and close to the expected emission peak of the strong emission line Fe II (74) λ6456. Its P-Cygni absorption component was distinct on March 19 and became flat-bottomed by March 22. The presence of this feature made it impossible to measure the absorption velocity of Hα any longer. All lines of Fe II strengthened with time.

Sc II has been identified by Patchett & Branch (1972) in SN 1959 in NGC 7331. We identify the absorption feature at $\lambda\lambda$5517–5513 seen first on March 4 with Sc II (29) λ5606. It became saturated by March 16.

3.2.5 *Lines due to Cα I and Ca II*

The infrared triplet of Ca II $\lambda\lambda$8498, 8542, 8662 was strong since the very beginning. Its P-Cygni absorption is affected by atmospheric H_2O bands, but it was possible to estimate its velocity as – 7900 km s^{-1} on March 3.62 and – 7700 km s^{-1} on March 5.62. The emission initially narrowed down (see Fig. 4), but later broadened again and began to show some structure by March 16. There were two emission peaks at λ8647 and λ8693. The peaks shifted to λ8666 and λ8716 on March 27.

The relative intensities of the three lines of Ca II is expected to be 1:9:5 in an optically thin case, *i.e.* a centroid wavelength of λ8579. The strong emission at wavelengths much larger than this suggests that there are other contributors to this blend. We suggest in the following subsection that N I is the principal contributor.

According to Kirshner *et al.* (1973) most of the calcium in SN envelopes is expected to be in the form of Ca II. However, one out of 10^4 atoms would still be neutral and thus show their presence particularly when Na I D line is strong and saturated. The likely lines are Ca I (1) λ4226 and Ca I (3) $\lambda\lambda$6127, 6166. Based on the absorption velocities we infer that the latter contributes to Fe II (74) λ6148.

3.2.6 *The Lines of C, N and O*

We have looked for the presence of C I and C II lines in the spectrum of SN 1987a, but could not identify positively even the strongest features expected.

The emission on the red wing of Ca II λ8600 is most likely N I (1) $\lambda\lambda$8680–8747 of which λ8680 is the strongest line. Fe I (60) $\lambda\lambda$8662, 8768 may contribute in this region at later stages; however, their presence is not very likely at the stage observed, since most of iron is in Fe II, and since other lines of the multiplet at $\lambda\lambda$8327, 8387 do not appear to be present. Further, the centroid of the emission was at λ8680 on March 30 suggesting that Ca II had faded considerably by then and the emission was largely due to N I λ8680 (see Fig. 7). The presence of these high-excitation lines in such a strength suggests that N I is overabundant, and hence that the material had undergone CNO-processing before ejection.

The emission due to O I λ7774 was visible on March 8, and was quite prominent on March 16 and 26. The blue-shifted absorption was clearly seen on March 26 at -2306 km s^{-1}.

4. The evolution of the photosphere

If SN 1987a were to exhibit a photometric behaviour typical of Type I or Type II Supernovae, one would have expected it to brighten to at least magnitude 1 at the distance of LMC. Though it brightened very rapidly on February 24, it lingered around $V = 4.5$ and then began to brighten slowly to $V = 4.0$ on March 24.

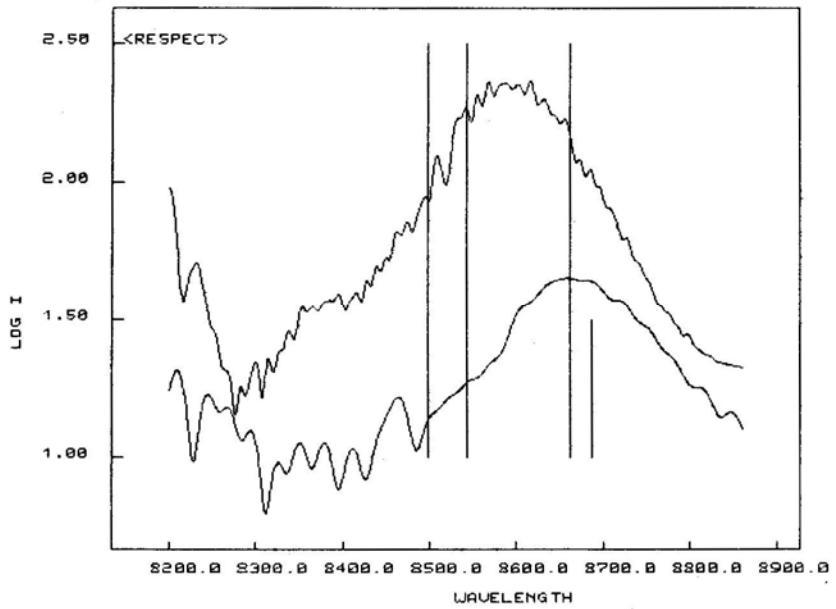

Figure 7. The region around Ca II λ86OO and N I λ8680 on 1987 March 8 (top) and March 30 (bottom). The longer vertical bars are at Ca II λ8498, 8542, 8662, whereas the shorter one is at N I λ8680.

We reproduce in Fig. 8 the *V* and *B* light curves and *U – B, B – V, V – R, V – I* colour curves for the period 1987 February 24–1987 March 25, based on the data published in IAU circulars. Also included is one estimate of *V* from VBO on March 6 (K. E. Rangarajan & K. Jayakumar 1987, personal communication) and a set of *V* magnitudes due to van Vuuren between March 15–21 (M. Feast 1987, personal communication). It is interesting to note that the *B* light curve follows the typical trend and reaches a plateau, but shows signs of further increase in brightness. The plateau is at a magnitude of 5.7, about 1.1 mag below the maximum of February 24. The colour gets redder at a high rate, the change between February 24 and March 24 being from – 0.8 to +2.2 in *U – B*, from 0.0 to 1.6 in *B – V*, from 0.25 to 0.7 in *V – R*, and from 0.35

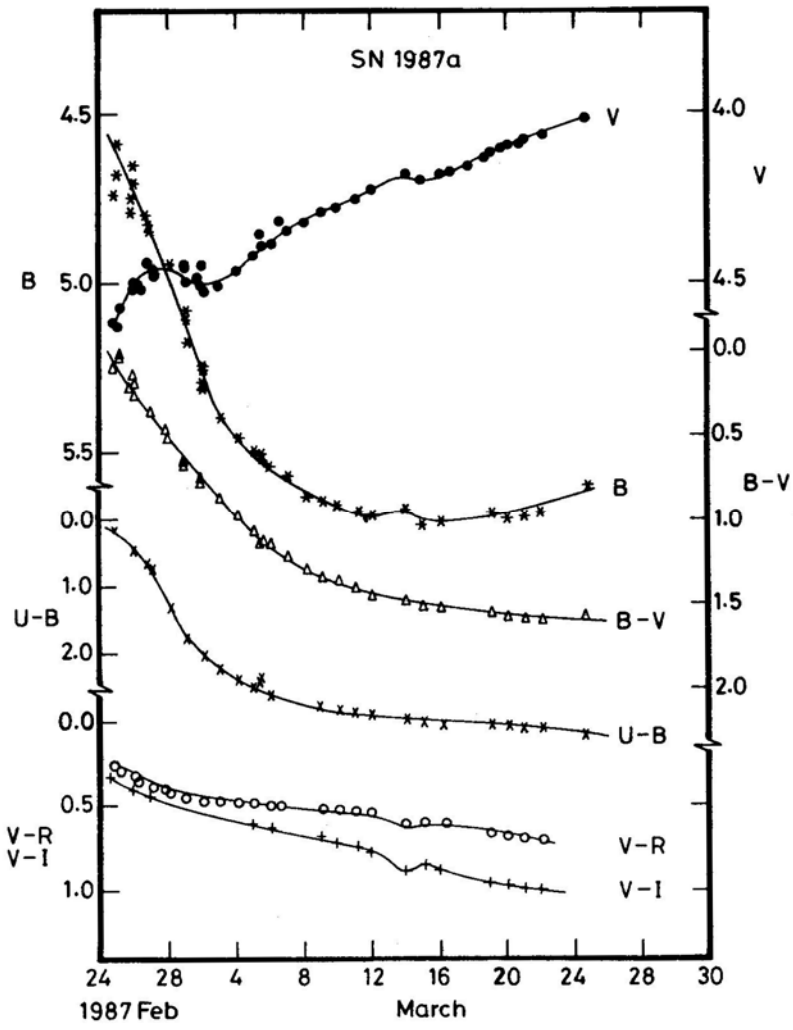

Figure 8. The *B, V* light curves, and *B – V, U – B, V – R, R – I* colour curves of SN 1987a based on the data compiled from various sources. The *R* and *I* bands are on the Cousins system.

to 1.0 in $V - I$ The light curve was hence rising in R and I bands as well, though dropped sharply in U and B before reaching a plateau at $U = 7.7$, $B = 5.7$.

Though this photometric behaviour is so atypical that it is difficult to predict its future course, it is instructive to compare it with the Type II supernova SN 1973r in NGC 3627, sometimes termed subluminous. SN 1973r reached a maximum at $V \simeq 14.2$ and $B \simeq 15.0$ on 1973 December 19. About a month later, the plateau was reached at $V \simeq 14.6$ and $B \simeq 6.5$ (Ciatti & Rosino 1977). Assuming a value of $E(B–V) = + 0.6$, the maximum and plateau correspond to $V_0 = 12.2$, $B_0 = 12.4$, and $V_0 = 12.6$, $B_0 = 13.9$ respectively. The change in $(B - V)_0$ ranges from 0.2 at maximum to 1.3 at plateau.

The distance modulus to NGC 3627 is 29.83 according to de Vaucouleurs (1979). Assuming a distance modulus of 18.5 for LMC, the magnitudes of SN 1973r translated to the distance of LMC would be $V_0 = 0.9$, $B_0 = 1.1$ at maximum, and $V_0 = 1.3$, $B_0 = 2.5$ at the plateau. Clearly, these values are much brighter than the range of magnitudes displayed by SN 1987a so far. On the other hand, the steep colour curve of SN 1987a resembles, to a great degree, that of SN 1973r.

The broad-band colours of SN 1987a can be compared with supergiants, and the effective temperatures determined. The V magnitudes and effective temperatures can be used to estimate the angular radii of the photosphere at different times. The known distance to LMC helps in converting the angular sizes to linear sizes. We have estimated photospheric temperatures by comparison with the colours and temperatures of supergiants as tabulated by Johnson (1967). The $(B - V)_0$ colours were used when $(B - V)_0 \lesssim 0.5$ and the $(V—R)_0$ colours were used above this value. The observed colours were corrected for interstellar extinction estimated as $E(B - V) = 0.17$ and $E(V - R) = 0.15$ using the photometric data on Sk – 69° 202.

The angular radii (θ) were determined using the calibration of Barnes, Evans & Parsons (1976):

$$\log \theta(\text{mas}) = 0.1864 - 0.2 V_0 + 0.855 (V - R)_0$$

The ratio $R = A_v / E(B — V) = 3.2$ was assumed to correct for interstellar extinction. The derived values of photospheric temperatures and radii are listed in Table 2 and plotted in Fig. 9. The radius increases from 4100 $R_\odot$ on February 24 to 17200 $R_\odot$ on March 22, while the temperature decreases from 10500 K to 4500 K. The kink on February 14 results from the hump in the V light curve and dip in $V - R$ colour curve on that day, which is based on a single observation, and hence may need confirmation (see, however, Section 5).

5. Discussion

We have assumed in the calculations of photospheric parameters that the supernova radiates like a supergiant. We believe that this is a better approximation than a blackbody. The available *UBVRI* data suggest that blackbody approximation held good during the early phases, except that the U magnitudes were fainter than predicted by blackbody because of blanketing effects. Also, the derived blackbody temperatures are somewhat higher than the supergiant temperatures in Table 2. As time progresses, it becomes more difficult to fit a blackbody spectrum, the B magnitudes also falling short of blackbody and the R and I bands showing an excess. The supergiant spectra, however, match the *UBVRI* data better all through.

Table 2. Photospheric temperatures and radii.

	Date 1987	V_0	$(B-V)_0$	$(V-R)_0$	Ref.	T_{eff} K	θ mas	$R/R_\odot$
February	24.8	4.09	−0.06	0.25	1	10500*	0.38	4100
	25.9	3.98	+0.06	0.31	1	8600*	0.45	4900
	26.8	3.90	0.19	0.35	1	7500*	0.51	5500
	27.1	3.92	0.21	0.42	2	7400*	0.58	6300
	28.1	3.93	0.22	0.48	2	7300*	0.65	7000
March	1.1	3.94	0.49	0.50	2	6400*	0.67	7300
	2.1	3.96	0.51	0.53	2	6300*	0.71	7600
	3.1	3.97		0.52	2	5800	0.69	7400
	4.1	3.93		0.53	2	5700	0.72	7700
	5.1	3.88		0.54	3	5700	0.75	8100
	6.1	3.84		0.55	3	5600	0.78	8400
	9.1	3.76		0.59	3	5500	0.87	9400
	10.1	3.74		0.60	3	5400	0.90	9700
	11.1	3.72		0.63	3	5300	0.96	10400
	12.1	3.69		0.63	4	5300	0.97	10500
	14.1	3.64		0.74	4	4900	1.24	13400
	15.1	3.66		0.70	4	5100	1.13	12300
	16.1	3.64		0.72	4	5000	1.19	12900
	19.1	3.58		0.79	4	4700	1.41	15200
	20.1	3.56		0.80	4	4700	1.45	15600
	21.1	3.54		0.83	4	4600	1.55	16700
	22.1	3.53		0.84	4	4500	1.59	17200

* Derived using $(B-V)_0$ colour.

References to the photometric data: 1. IAU Circular No. 4352; 2. IAU Circular No. 4332; 3. IAU Circular No. 4341; 4. IAU Circular No. 4352.

Extinction corrections applied: $E(B-V)=0.17$, $E(V-R)=0.15$, $A_V = 0.54$.

$(V-R)$ was transformed from Cousins system to Johnson system using transformations of Taylor (1987).

Inclusion of infrared data helps fitting blackbody curves (*of.* Bouchet *et al* 1987) better. However, the increase in bolometric luminosity may not be as fast as predicted by the blackbody fits. The energy integrated over *UBVRI* bands was 3.1×10^{-10}, 3.1×10^{-10} and 6.2×10^{-10} Wm^{-2} on February 24, March 11 and March 22 respectively. These variations are much smaller in magnitude compared to the variations in total luminosity derived by Bouchet *et al.* between March 1–11 using blackbody fits. Actually, during the latter period, there is a slight fall in the total *UBVRI* flux because of decreasing light in *U* and *B.*

The values of radius and temperature derived in Table 2 are based on *V* light and $V-R$ colour, and would represent the region of wavelengths where the bulk of the energy is radiated. The derived photospheric radii yield a photospheric velocity of 4200 km s^{-1} between February 24 and March 22, consistent with the observed absorption velocities of lines other than hydrogen.

The development of the spectrum of SN 1987a is consistent with the changes in colour and temperature derived from photometry: The continuum energy distribution generally gets redder with time. The evolution in radius and temperature is not smooth; there are kinks around March 3 and March 14. In the latter case, the radius increased faster than usual whereas the temperature decreased. This coincides with a slight enhancement of lines due to neutral metals like Ca I, and the emergence of Fe II λ6456.

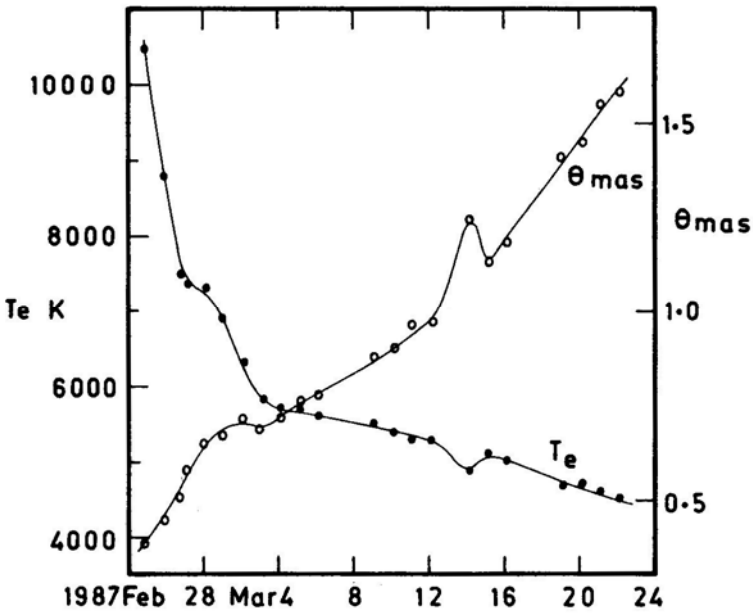

Figure 9. The variation of temperature and angular radius of the photosphere of SN 1987a as a function of time.

The radial velocities of the Na I D feature seem to show a higher value around this time. Such a behaviour is not obvious in the case of Fe II lines.

The radial velocities of the blueshifted absorptions show a redward movement and reach a plateau around March 22 in the case of most of the Fe II lines and possibly also in the case of Na I. The radial velocity of the Hα absorption core starts with a larger magnitude and decreases analogously. It is difficult to estimate its value after March 19 because of the emergence of Fe II λ6456. If the dip seen at λ6487 on March 25 is attributed to the absorption of Hα, the implied velocity is –2673 km s^{-1} which is about the value shown by the Fe II lines. The variation of absorption velocities is consistent with the picture of an expanding, scattering envelope with velocity increasing with distance above the photosphere and the optical depth reducing with time.

Although the *V* light as well as the bolometric luminosity are increasing, the spectrum is getting later and later. Many lines of Fe II and Na I show flat-bottomed absorption indicative of high optical depths in the lines.The similarity with SN II 1973r in NGC 3627 (Ciatti & Rosino 1977) mentioned in Section 4 appears to extend to the spectroscopic evolution too; however, the process is more rapid in SN 1987a and the Fe II lines are much stronger than seen in SN 1973r.

A comparison can be made of SN 1987a with Type II SN 1979c in M100 at a stage when the metallic lines were well developed, and when the photospheric temperatures are roughly the same, i.e., roughly a month after the light maximum of SN 1979c (1979 May 28). Though our spectra of SN 1987a were obtained before the maximum in *V* light, the similarity of the spectra suggests that the physical conditions in the atmosphere of SN 1987a had already reached by March 8 the conditions in SN 1979c

on May 28. The spectrum of 1979c was also matched by Branch *et al.* (1981) with a synthetic spectrum computed by assuming solar abundances and that the lines are formed in a scattering, spherically symmetric, expanding atmosphere with a photosphere that emits like a blackbody. According to Branch *et al.*, the spectrum of SN 1979c was characterized by $T_* \simeq 6000$ *K* and $V_{\exp} \simeq 8000$ km s^{-1} on May 26. In the case of SN 1987a, the Hα velocity is 8000 km s^{-1} and $T_* \simeq 5600$ K around 1987 March 8 and 9. A closer look at the spectra shows that the Fe II and Na I lines were much stronger in SN 1987a than both observed and synthesized ones in SN 1979c, indicating higher optical depths in these lines of SN 1987a. Branch *et al.* estimate the mass of the scattering envelope of SN 1979c as $\simeq 0.58\ M_\odot$. In order to produce higher optical depths in the case of SN 1987a one would require $\gtrsim 0.58\ M_\odot$ of envelope mass, provided the abundances are the same in both the Supernovae (relative to H). It is possible to reduce this limit slightly if the metal abundance is lower in SN 1987a. In such an event, the electron density reduces and consequently so does the continuum opacity. As a result, the contrast between the lines and the continuum will also increase resulting in stronger lines. A more quantitative study is needed to estimate the envelope mass accurately.

Acknowledgements

We would like to express our thanks to many people for their encouragement. Particular thanks are due to Prof. J. C. Bhattacharyya, and several colleagues for generous donation of the 40-inch telescope time for this programme. We thank Dr Sushma Mallik for obtaining some of the spectra and Mr A. Jairaj for digitizing the spectrograms with the PDS microdensitometer. The digital reductions were carried out using the VAX 11/780 systems at VBO, Kavalur, and Raman Research Insitute, Bangalore.

References

Barnes, T. G., Evans, D, S., Parsons, S. B. 1976, *Mon. Not. R. astr. Soc*, **174,** 503.
Beer, A.1973, *Vistas Astr.*, **16**, 179.
Branch, D., Falk, S.W., McCall, M. L, Rybski, P., Uomoto, A. K., Willis, B. J.,1981, *Astrophys. J.*, **244,** 780.
Branch, D., Lacy, C. H., McCall, M. L, Sutherland, P.G., Uomoto, A., Wheeler, J. C, Willis, B. J. 1983, *Astrophys. J.*, **270,** 123.
Bouchet, P., Stanga, R., Le Bertre, T., Epchtein, N., Hamann, W. R., Lorenzetti, D. 1987, *ESO Scientific Preprint* No. 500.
Ciatti, F., Rosino, L. 1977, *Astr. Astrophys.*, **56,** 59.
de Vaucouleurs, G. 1979, *Astrophys. J.*, **277,** 729.
Johnson, H. L.1967, *A. Rev. Astr. Astrophys.*, **4**, 193.
Kuan, P., Kuhi, L. V, 1975, *Astrophys.* J, **199,** 148.
Kirshner, R. P., Oke, J. B., Penston, M. V., Searle, L. 1973, *Astrophys. J.*, **185,** 303.
Patchett, B., Branch, D. 1972, *Mon. Not. R. astr. Soc*, **158,** 375.
Prabhu, T. P., Anupama, G. C, Giridhar, S. 1987, *Bull astr. Soc. India*, (submitted).
Rottenberg, J. A. 1952, *Mon. Not. R. astr. Soc*, **112,** 125.
Taylor, B. J. 1986, *Astrophys. J. Suppl. Ser.*, **60,** 577.